Colloid Polym Sci 278:104–113 (2000)

ORIGINAL CONTRIBUTION

R. Johann
D. Vollhardt
H. Möhwald

Faceting of monolayer domains

Received: 9 August 1999
Accepted in revised form: 24 August 1999

Presented at the 39th General Meeting of the Kolloid-Gesellschaft, Würzburg, 27–30 September 1999

R. Johann (✉) · D. Vollhardt
H. Möhwald
Max-Planck-Institute of Colloid
and Interface Science, D-14476 Golm,
Germany
e-mail: johann@mpikg-golm.mpg.de
Tel.: +49-331-5679461
Fax: +49-331-5679202/+49-331-5679222

Abstract The formation of facets in domains of three monolayer systems, differing in molecular structure or headgroup charge, is observed by Brewster-angle microscopy under different experimental conditions. Arachidic acid forms faceted domains on increasing the pH of the subphase from pH 12.0 to 12.3 or by adding traces of cholesterol at pH 12.0. The degree of faceting is gradually varied in a mixture of 1-monopalmitoyl-*rac*-glycerol and 1-*O*-hexadecyl-*rac*-glycerol. The surface potentials of the pure substances were measured in order to determine the electrostatic forces in the mixture. Reversible faceting of domains of heptadecanoic acid methyl ester is observed within 2 °C near 30 °C. Faceting in monolayers is explained on the basis of fundamental forces that govern domain texture and shape, including line tension anisotropy and electrostatic repulsive forces. This explanation also accounts for the formation of dendrites along certain directions at domains of arachidic acid and the methyl ester.

Key words Facets · Domain shape · Monolayer · Line tension anisotropy · Arachidic acid

Introduction

The peculiar property of an air–water interface to uniformly orient amphiphilic molecules leads to a unique phase behaviour of the matter accumulated there. Dipolar interactions, originating from this interfacial asymmetry, contribute to the variety of the shapes of the domains that emerge in the main phase transition of several monolayer systems. The domain shape often depends sensitively on the temperature, the chemical composition, the subphase and the relative portions of the two coexisting phases.

There are two independent approaches for interpreting domain features. The first one is derived from the observation by fluorescence microscopy that there are two phases in the coexistence region, both of which appear to be homogeneous and isotropic . It considers the interplay between line tension and electrostatic repulsion [1] and is similar to the treatment of thin films of a ferromagnetic fluid within a nonferromagnetic fluid [2]. The second approach [3, 4] tries to explain the inner structure of domains as detected by polarized fluorescence microscopy and Brewster-angle microscopy and is based on the continuum elasticity theory developed for smectic liquid crystals [5]. A comprehensive theory, however, that is able to account for the various domain types and textures that exist and which combines the elements of both approaches is still to be expected.

There are monolayers which form domains with sharp edges and corners that look like two-dimensional crystals with facets. Facets usually reflect a regular lattice and long-range positional order, which, however, is not possible in one or two dimensions. Their appearance in monolayers, is therefore, not yet completely understood [6]. With three selected monolayer systems as examples that form polygonal domains under different experimental conditions, an explanation for facet formation is offered that relies on the fundamental forces governing domain features. As equilibrium is required for those to be applied, the question of possible effects connected with domain growth is of crucial importance.

Forces governing domain texture and shape

A monolayer consists of an array of dipoles with a component normal to the monolayer plane. In the coexistence region of the main phase transition the charge and the dipole density of the LC phase domains and the LE phase are different. This leads to long-range repulsion between the domains preventing them from fusing, and a hexagonal superlattice is formed [7]. The repulsive dipolar interaction of the molecules within a domain favours a large boundary-to-area ratio, by which the electrostatic energy is reduced. It is thus opposed to the line tension that tends to preserve the circular shape. The free energy of an isotropic domain has the form [8, 9]

$$F = F_{\mu} + F_{\lambda} = I\mu^2 + P\lambda \ . \qquad (1)$$

μ is the difference in dipole density between the LE and the LC phase, $I\mu^2$ is the integral of the electrostatic energy between all dipoles in the domain (I just depends on the domain shape), P is the domain perimeter and λ is the line tension. The electrostatic forces increase with domain size and at a critical area they become unstable and form ellipses [10], stripes [11] or higher harmonic shapes [12]. Regarding the texture of domains one may write

$$F = \int \left[\frac{K_{\mathrm{s}}}{2} (\nabla \cdot \mathbf{c})^2 + \frac{K_{\mathrm{b}}}{2} (\nabla \times \mathbf{c})^2 \right] \mathrm{d}x\, \mathrm{d}y (1) + F_{\mathrm{def}}(2) + L\varepsilon(3) + \oint \sigma\, \mathrm{d}l (4) \ . \qquad (2)$$

The numbers in parentheses behind each energy term denote the part of the domains in Fig. 1, the energy of which is described by the corresponding term. The brackets contain the two second-order terms of the Landau expansion for describing the bulk elasticity. These terms account for the energy cost of distortions in the long-range tilt order and the underlying lattice that is strongly coupled to the tilt. This expression was originally applied to textures in smectic liquid crystals [12] and it is also consistent with the symmetry of monolayer phases [13]. $\nabla \cdot \mathbf{c}$ is a splay distortion with $\mathbf{c}$ being a unit vector order parameter that points along the projection of the molecule onto the x-y plane (Fig. 1a). A splay motif would exist if all the molecules were tilted along the radial directions emerging from the centre of a circle with all chain ends pointing in the same direction. The motif of $\nabla \times \mathbf{c}$, the bending distortion, is a set of concentric circles where all molecules are uniformly aligned on the circumference. In domains both motifs are often superimposed. The first-order term for splay is allowed for Langmuir monolayers but not for smectic liquid crystals due to broken inversion symmetry in monolayers. For systems large compared to the molecular size higher-order terms can be neglected. The linear term for splay can be included in the line energy via Gauss law and the term for bending is zero for achiral molecules (since the rotation changes sign when aligning the molecules once clockwise and once counterclockwise on the circle of the bending motif mentioned, where there should be no energy difference for achiral molecules). The factors K_{s} and K_{b} are a measure of the elasticity of the phase. The most favourable state is

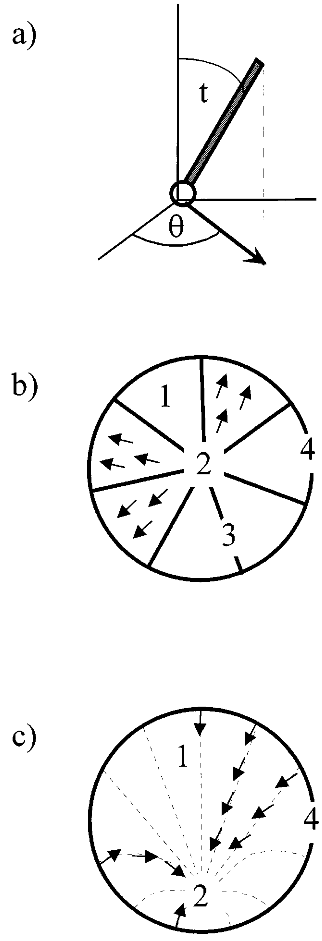

Fig. 1 a The orientation of a molecule is defined by the tilt angle, t, and the azimuthal angle θ. The unit vector $\mathbf{c}$ lies in the monolayer x-y plane on the projection of the molecule onto this plane pointing towards the tail end; $\mathbf{c} = \mathbf{x} \cos\theta + \mathbf{y} \sin\theta$. Two textures representing basic features encountered in monolayer domains are **b** a domain with segments of uniformly aligned molecules and **c** a boojum pattern as observed for domains of pentadecanoic acid with splay and bending and without defect lines. The *numbers* refer to the energy terms of Eq. (2)

reached when all molecules are aligned parallel, where the expression becomes zero. F_{def} is the energy of the point defect which is mostly found in the middle or at the edge of the domain; it depends on the number of defect lines crossing this point [4]. The energy of the defect lines is proportional to the overall length L (term 3). In continuum elasticity theory [4] it is assumed that the pseudohexagonal lattice continues across the boundary between two segments of different tilt. The defect arm is considered as a narrow region where the tilt azimuthal angle has to pass several energy minima, when it jumps to exactly 60° corresponding to the angle between neighbouring hexatic bond directions. However, as numerous domains have been observed, the inner structures of which do not comply with this theory (jumps in angle at the segment boundary different from 60°) it might be more reasonable to assume that the segment boundaries correspond to grain boundaries with high defect concentration, and so the lattice correlation is weak. While the bond order might be short ranged near the boundary, the tilt orientational order continues to exist. At the segment edge the molecules abruptly change their orientation and create a sharp bondary line. Its energy may depend on the angle the tilted molecules of a segment make with the boundary and possibly on the angle they make with the molecules at the border of the neighbouring segment. Term 4 is the energy of the closed boundary line of the domain. The line tension σ, is developed into a Fourier series $[\sigma(0) = \sigma(2\pi)]$

$$\sigma = \lambda_0 + \lambda_1 \cos\varphi + \lambda_2 \cos 2\varphi + \cdots \tag{3}$$

λ_0 is the isotropic line tension and λ_1 and λ_2 are the anisotropic line tensions. φ is the angle between the director, **c**, and the surface normal, **n**. The sine terms are omitted, since there is no difference in line tension if the molecule is tilted to one side (φ_1) or to the opposite side ($-\varphi_1$) of the surface normal when chiral interactions are absent. A normal boundary condition with the tilt direction outwards or inwards towards the defect core is mostly observed (Fig. 1b, c). However, there are also cases with molecules being pinned parallel to the boundary [12, 14]. The origin of boundary pinning is not yet clear. With parallel alignment φ is the angle between the surface element **dl** and **c** [12]. The dominance of the boundary energy increases with domain size as the gradient terms in term 1 scale independently of the radius.

According to simulations of the pentadecanoic acid boojum texture by Loh and Rudnick [15] the experimentally observed shape can be explained by line tension anisotropy alone. The relative values of K_s and K_b seem to be of minor importance. Rivière and Meunier [13] found a higher value of K_s for the boojum, despite the fact that almost only splay and little bending are observed. From this they concluded the prominent role of the boundary conditions.

The equilibrium texture, of course, corresponds to the minimum of F. So some qualitative conclusions on the development of domain textures can be drawn. With regard to the bending energy a domain would have the lowest energy when the tilt of all molecules has the same direction. The line tension anisotropy, however, tends to orient the molecules at the boundary, say, normal to it. This causes a bending in the molecular orientations and an increase in bulk energy, while boundary strain is released; so a boojum pattern is formed. If the phase, however, is too rigid, i.e. K_s and K_b are too high, then a favourable solution appears to be the formation of defect lines that separate the bulk into several segments in each of which the molecules are aligned parallel and boundary strain can be kept small. The latter decreases with the number of defect lines and the consequent increase in defect line energy. It may also occur that a certain tilt angle at the segment boundary is preferred. If this angle does not coincide with half the segment angle, it can only be set and the defect line energy can only be lowered by producing bending within the segment. By shifting the defect point from the domain centre to the edge, the energy of the defect point as well as the overall length of the defect lines become smaller. Furthermore the angle between two defect lines is not restricted anymore to a fixed value. In contrast the anisotropic boundary energy is enhanced compared to centred domains.

Materials and methods

Arachidic acid (AA) (eicosanoic acid) was obtained from Merck. 1-*O*-hexadecyl-*rac*-glycerol (ETD), 1-monopalmitoyl-*rac*-glycerol (ESD), heptadecanoic acid methyl ester and cholesterol were purchased from Sigma. The substances were dissolved in a mixture of *n*-heptane (for spectroscopy, Merck) with 5% ethanol (p.a., Merck) without further purification. AA was spread on the alkaline subphase. The pH of the subphases was adjusted with NaOH (1 M Titrisol, Merck). To remove traces of polyvalent cations, 10^{-4} M ethylenediaminetetraacetate (99.9995%, Aldrich) was added. A Brewster-angle BAM2 microscope from NFT (Göttingen) fixed on a homemade trough with a continuous Wilhelmy-type pressure measuring system was used to image the surface with a resolution of 4 μm. The brightness and contrast of the images could be improved with image-processing software.

Surface potential measurements were performed using the vibrating capacitance technique. A measuring apparatus (KSV Instrumente) with a conducting vibrating plate of about 4-cm in diameter was used. The temperature was determined with an accuracy of better than ±0.5 °C.

Results

Monolayers of long-chain fatty acids that are condensed and coexist with the gas phase at zero surface pressure on a neutral subphase develop a plateau at high pH values. The onset of the plateau corresponds to the formation of LC domains in a first-order phase transition [16]. For AA, domains with smooth and nearly circular shape are obtained at pH 12.0. With an analyser in the beam path three different texture types are revealed that are distinguished by the number of segments and the location of the defect point. One type has a defect point in the domain centre which is enclosed by six segments of nearly equal size (Fig. 2a). Within a segment the molecules are aligned uniformly and at the boundary to a neighbouring segment the tilt direction changes discontinuously. When the pH of the subphase is increased to 12.3 polygonal domains grow with sharp corners and straight edges or edges with relatively low curvature (Fig. 2b). They look like two-dimensional crystals with facets, while the inner domain structure is identical to that at pH 12.0. The curvature of the domain boundary can vary according to the pH conditions. When the film is left to stand for more than 2 h the degree of faceting continuously decreases and finally the circular form is recovered due to the action of atmospheric carbon dioxide which reduces the pH of the subphase [16].

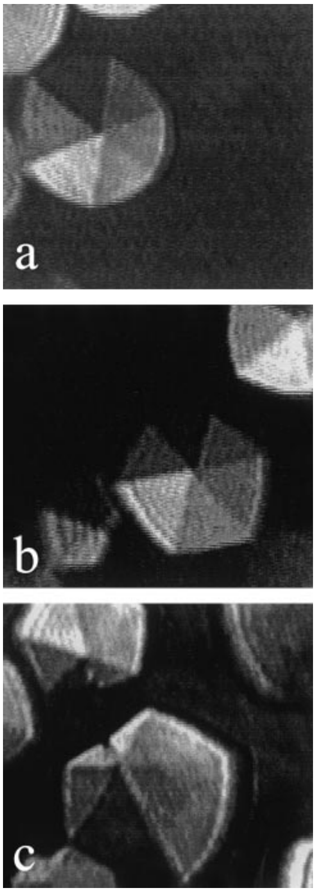

Fig. 2 Domains of arachidic acid grown on an alkaline subphase at **a** pH 12.0 and **b**, **c** pH 12.3 with hexagons and pentagons coexisting; the latter domains are also obtained with 1 mol% cholesterol at pH 12.0; 25 °C, 0.03 $\mathrm{nm}^2\,\mathrm{mol}^{-1}\,\mathrm{min}^{-1}$, 165 × 180 $\mu\mathrm{m}^2$

In order to examine whether the faceted forms are equilibrium forms the domains were grown at pH 12.0 or 12.3 and kept between fixed barriers and then the pH of the subphase was increased or reduced by addition of base or acid. Simultaneously, the change in shape was observed. The transformation between rounded and faceted shape was found to be gradual and reversible with variation of pH. Around pH 12 the condensed phase of AA has not yet completely deprotonated [17]. On increasing the pH from 12.0 to 12.3 the degree of dissociation rises, leading to higher electrostatic repulsion between the carboxylic headgroups. The electrostatic energy that has to be overcome on condensation produces a shift in the phase-transition pressure to higher values (Fig. 3) [18] (a doubling of the sodium concentration alone at pH 12.0 was not found to be responsible for this increase in plateau pressure). Faceted domains can also be grown on a subphase of pH 12.0 when 1 mol% cholesterol is added to the spreading solution of AA. Cholesterol has been observed to reduce the line tension of lipid domains [19].

In order to disclose the origin of faceting further substances were looked for, the domains of which could be transferred into the faceted forms by applying conditions that lead to an increase in the electrostatic repulsion between the domain molecules or to a decrease in the line tension.

ESD and ETD represent very similar molecules that differ only in that instead of the ester group in ESD there is an ether group in ETD. Pure ETD forms facets above 30 °C and on cooling the shape distorts while the texture develops splay and bending. The elongations become thinner with falling temperature [20]. This behaviour is

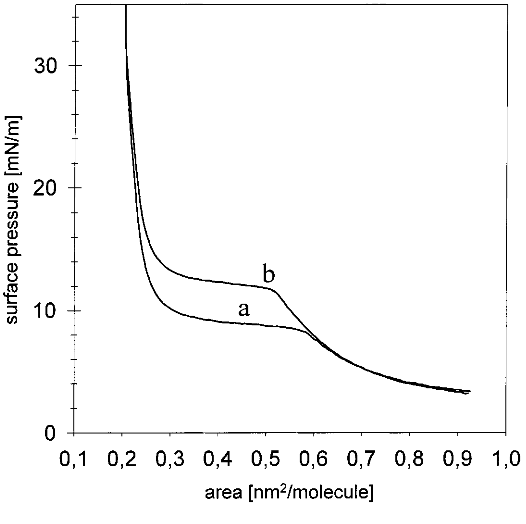

Fig. 3 π–A isotherms of arachidic acid at **a** pH 12.0 and **b** 12.3; 25 °C, 0.03 $\mathrm{nm}^2\,\mathrm{mol}^{-1}\,\mathrm{min}^{-1}$

contrast to that of pure ESD, which forms circular domains at all temperatures, and even the addition of cholesterol has no effect. This indicates higher electrostatic interactions or a lower line tension for ETD than for ESD. Surface potential measurements of pure ETD and ESD reveal that the difference in dipole density, μ, of the coexisting LE and LC phases is much larger for ETD than for ESD (Fig. 4). After the kinks in the surface potential curves, that coincide with the beginning of the plateau in the surface pressure–area isotherms, there is a short linear region for both ETD and ESD. In this part the potential follows the lever rule and corresponds to the sum of the contributions of pure LE and LC phase with $\Delta V = \Delta V_{\mathrm{LE}} x_{\mathrm{LE}} + \Delta V_{\mathrm{LC}} x_{\mathrm{LC}}$ (ΔV_{LE} and ΔV_{LC} are the potentials of the pure LE and LC phases). This is used as the basis to determine the difference in the potentials of the two phases by extrapolating a straight line from A_{LE} to A_{LC} (see Fig. 4) [21]. With $\Delta V = p/\varepsilon\varepsilon_0$ (p is the molecular dipole moment per molecular area and $\varepsilon\varepsilon_0$ is the absolute dielectricity constant) $\Delta V_{\mathrm{LE}} - \Delta V_{\mathrm{LC}}$ is directly proportional to μ ($\mu = p_{\mathrm{LE}} - p_{\mathrm{LC}}$). From at least four measurements with both ESD and ETD $\Delta V_{\mathrm{LC}} - \Delta V_{\mathrm{LE}}$ was found to be between 100 and 170 mV for ETD and between 3 and 14 mV in the case of ESD. Now mixtures were prepared from ETD:ESD ratios of 60:40 to pure ETD in order to continuously vary the magnitude of the forces and to observe the change in domain shape. ETD and ESD are miscible above an ETD:ESD ratio of 50:50 [22]. Figure 5 demonstrates the gradual increase in the faceting of domains grown to about the same mean molecular area, when the portion of ETD is raised. At about 60% ETD the domains still appear rounded as in pure ESD (Fig. 5a). As the amount of ETD is increased the curvature of the boundary at each of the seven segments reduces (Fig. 5b) until faceting is complete with pure ETD (Fig. 5c).

In each case irregular domains formed at high compression rates relax immediately into the stable growth forms shown. Consequently these shapes, which developed at a slow rate, represent the equilibrium forms. In the third example domains of heptadecanoic acid methyl ester were exposed to a change of temperature. Circular domains of the ester, to which 0.8 mol% cholesterol was added, were grown at 32 °C and then cooled to 27 °C. Within only 2 °C from 29 to 27 °C faceting became more and more pronounced and eventually dendrites emerged along the segment bound-

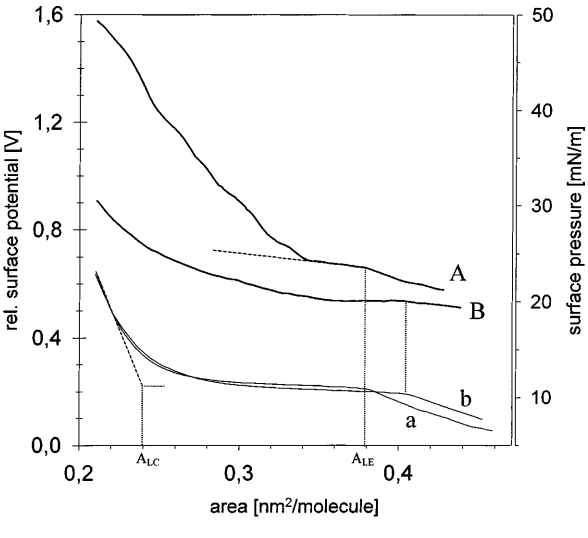

Fig. 4 Surface potentials (*upper curves*) and π–A isotherms of 1-*O*-hexadecyl-*rac*-glycerol (*ETD*) (*A*, *a*) and 1-monopalmitoyl-*rac*-glycerol (*ESD*) (*B*, *b*) at 29 °C. The potentials are not absolute values and the potential curves for ETD and ESD do not correspond to each other. The differences in the potentials of the pure Liquid expanded (*LE*) and Liquid condensed (*LC*) phases are determined by extrapolating the linear part of the curves from A_{LE} to A_{LC} as sketched for ETD. A_{LE} is molecular area of the pure LE phase at the onset of the plateau and A_{LC}, the molecular area of the condensed phase, is obtained by extrapolating the steep part of the isotherm at low molecular area to the onset plateau pressure; compression rate: 0.02 nm^2 mol^{-1} min^{-1}

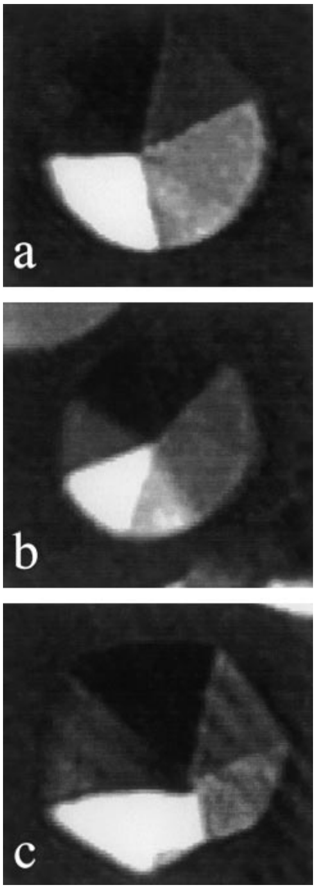

Fig. 5a–c The degree of faceting is gradually increased on increasing the portion of ETD in domains of a mixture of ETD and ESD. **a** ETD:ESD 65:35, **b** 85:15, **c** 100:0; 31.5 °C, 0.01 nm^2 mol^{-1} min^{-1}, 150 × 165 μm^2

aries, while the domain stretched. The dendrites and the domain body distort to fine stripes from which further arms sprout (Fig. 6).

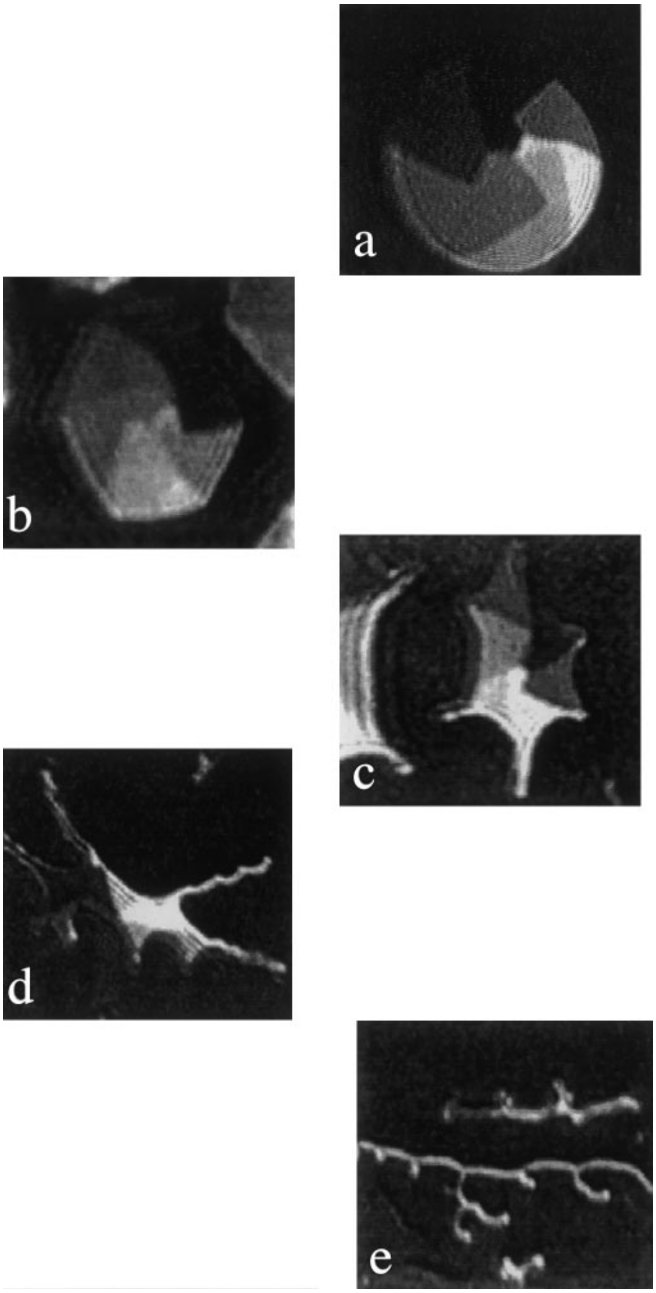

Fig. 6 a Domains of heptadecanoic acid methyl ester at 32 °C. Between 29 and 27 °C shape transformation begins with continuous faceting. The completely faceted state (**b**) is passed by forming dendrites at the edges of the segments with slightly negative curvature (**c**). Looking like waves the dendrites elongate and the domain body stretches (**d**). Eventually stripes develop with equidistant branching (**e**); a completely stretched domain is visualized in the *upper half* of the image. The spreading solution contained 0.8 mol% cholesterol

The transformation is completely reversible and upon heating the droplets and their texture are reformed. The temperature range of shape transformation depends very sensitively on the amount of cholesterol added. Below 0.5% complete faceting was not achieved on cooling and above 1% the domains deteriorate so quickly that intermediate states could not be observed.

The corresponding isotherms between 27 and 32 °C are presented in Fig. 7. At 27 °C the monolayer is condensed at zero surface pressure. Between 27 and 29 °C there is no measurable increase in pressure, but the higher compressibility at 29 °C indicates the existence of a very low plateau. In order to observe a pattern that deviates from circular for AA at pH 12.0, very high compression rates of around 0.70 $nm^2\ mol^{-1}\ min^{-1}$ are required. The boundary of the domains grown under this condition is irregular but relatively smooth (Fig. 8a). It contains notches and cusps, but distinguished growth directions do not appear. The inner domain structure, however, is faultless. The relaxation process is very fast (less than 1 s) and ends up with the circular form. If the pH of the subphase is changed to 12.3 and the same compression conditions are applied, domains develop, the shape of which is distinctly different from that at pH 12.0. When the defect lines cross in the domain centre and growth is uniform, six arms emerge radially from the domain centre pointing in the six symmetry directions, which gives the domains a starlike appearance (Fig. 8b). The dendrites grow along the segment edges prolonging the defect lines.

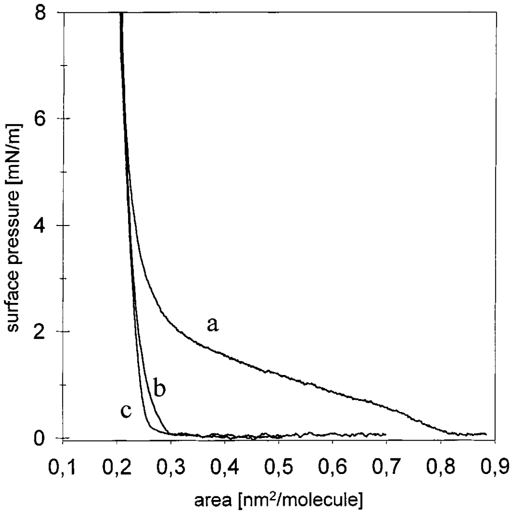

Fig. 7 π–A isotherms of heptadecanoic acid methyl ester with 0.8 mol% cholesterol at 32 °C (*a*), 29 °C (*b*) and 27 °C (*c*). The enhanced compressibility at 29 °C indicates the development of a plateau. At 32 °C the plateau appears at about 0.5 $mN\ m^{-1}$ at 0.74 $nm^2\ mol^{-1}$; 0.02 $nm^2\ mol^{-1}\ min^{-1}$

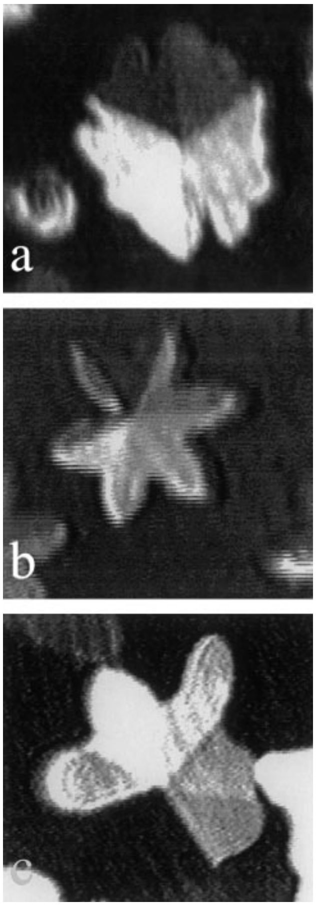

Fig. 8 Nonequilibrium growth of arachidic acid at **a** pH 12.0 and **b** pH 12.3, 28 °C, 0.7 $\text{nm}^2\ \text{mol}^{-1}\ \text{min}^{-1}$ and of **c** ESD, at 31.5 °C, 0.04 $\text{nm}^2\ \text{mol}^{-1}\ \text{min}^{-1}$; $185 \times 205\ \mu\text{m}^2$

It is worth noting that also in this case the texture is perfectly developed. Despite the extreme compression conditions, where the time for a domain to be grown to visible size is of the order of seconds, there is no difference in texture compared to that observed upon entering the plateau at a low rate. This indicates that the process of setting up the inner domain structure, i.e. the building up of the long-range tilt order and the arrangement of the defect lines, is a very quick one. It appears to be independent of kinetic and growth effects and, hence, is governed only by the forces described at the beginning, leading to equilibrium.

The relaxation into the compact faceted shape is accompanied by a decrease in the energy of the boundary line and the defect lines both reduce. At pH 12.3 the relaxation is slower than at pH 12.0 and needs about 20 s. The fact that it ends at the faceted form indicates that the equilibrium state is reached.

For comparison a nonequilibrium shape of ESD is shown in Fig. 8c. At a much lower compression rate the seven segments swell and protrusions emerge from the middle of each segment in contrast to AA at pH 12.3. An explanation for this varying behaviour is offered in the Discussion. By an analysis of the distribution of the shades of grey within a domain with respect to the plane of the incident laser beam and the analyser position, it is found for all domains presented in this paper that all the molecules within a segment are tilted towards the domain boundary.

Discussion

It was demonstrated that faceting occurs with rather different substances and under various conditions. This indicates the action of fundamental forces and it is unlikely that the facet formation is a consequence of peculiar chemical properties or certain experimental conditions, which would refer to a special phase, etc. There have been attempts to account for this phenomenon in monolayers [23–25]. One commonly assumes that faceting reflects the molecular order of the condensed phase as in three-dimensional crystals. Also, according to the hexagonal symmetry of the hexatic phase, for which the formation of facets should, in principle, be possible [6], one would expect patterns like those shown in Figs. 2b and 6b. There are, however, many instances for domains exhibiting facets, but with a symmetry deviating from hexagonal like that in Fig. 2c showing pentagons or like that in Fig. 5b with sevenfold symmetry. Thus there must be a different origin.

Qiu et al. [26] described the reversible transition of long-chain methyl esters from round to hexagonal when the phase boundary between the LS[1] phase with upright chains and the L_2' phase with tilted chains is crossed on varying the temperature. This suggests that the molecules must be tilted for faceting to be possible.

The reversible shape transformations of AA between pH 12.0 and 12.3 and the methyl ester within a small temperature range and the kinetic behaviour of AA and the ETD/ESD mixtures provide evidence that faceting is not caused by preferred kinetic growth at the domain corners and hindered relaxation as claimed by Berge et al. [23], but corresponds to a state of lowest energy. Faceting of the domains can be considered as the result of the lowering of curvature and the stretching of the boundary line of each segment within the domain, while the area of one segment and of the domain on the whole remains constant. Hence the facet orientation need not comply with the bonding symmetry.

In the mixtures of ETD and ESD facet formation is accompanied by an increase in the electrostatic repulsion between the domain molecules as the fraction of ETD and hence μ is increased. μ is the difference between the

---

[1] LS: phase name according to phase nomenclature for fatty acids (and derivatives)

dipole densities of the LE and LC phases and can be regarded as the effective dipole moment per unit area in the LC domains. Heptadecanoic acid methyl ester with a trace of cholesterol forms facets on decreasing the temperature from 29 to 27 °C. As the temperature is lowered, the onset of the main phase transition is shifted to higher molecular area. The molecular and dipole moment densities of the LE phase are reduced and with a constant density of the LC phase and minute or cancelling changes in the molecular dipole moments in the two phases with temperature assumed, μ also increases.

In the case of AA, μ contains contributions from changing the degree of dissociation. The change in excess charge corresponds to a change in dipole moment at relatively high counterion concentrations [27]. From the increase in transition pressure with pH (Fig. 3) only the increase in the charge density of the whole monolayer can be inferred. No information is obtained on the dipole densities of the coexisting phases. Owing to the fact that the expanded part of isotherms is independent of the pH but varies inversely with ionic strength, it was suggested that the LE phase is completely dissociated [28]. Then an increase in the plateau pressure with increasing pH must be caused by increased dissociation of the condensed phase. This, however, would approximate the dipole densities of the coexisting phases and reduce μ.

As mentioned at the very beginning, electrostatic forces favour a large ratio of domain boundary to area. Let us consider a domain in which line tension and electrostatic forces are in equilibrium. If now a new μ is imposed, the domain will relax and change its shape until the line tension and the electrostatic forces have again equilibrated. Each state of the continuous shape transformation from circular to faceted represents the state of lowest energy where the two forces balance each other with $\mathrm{d}F_\lambda = -\mathrm{d}F_\mu$. By using Eq. (1)

$$\mathrm{d}F = 0: \quad \mu^2 \mathrm{d}I = -\lambda \mathrm{d}P \ . \tag{4}$$

At a certain state the ratios $-\mathrm{d}I/\mathrm{d}P = \lambda/\mu^2$ have a defined value, c. One state may be described by $\lambda/\mu^2 = c1$ and the second one with a new μ' and the same λ as $\lambda/\mu'^2 = c2$ with $\mu' = a\mu$ (a is a constant). The same state may also be obtained by changing λ and keeping μ fixed. Thus a change in μ by a is physically equivalent to a change in λ by $1/a^2$.

At the transition from a circle to a regular hexagon the boundary expands by 5%. If μ is large enough as for the methyl ester, thin stripes can be produced. But why do the domains form facets and not an irregular or modulated boundary? The reason for this may be found in the domain texture. The molecules are all aligned parallel in each segment and no splay or bending is observed. As the textures of the rounded and faceted forms coincide, the defect point energies are equal. So the shape transformation only concerns the last two energy terms of Eq. (2). The electrostatic energy and the line energy (Eq. 3) may be combined as follows

$$\sigma' = \lambda_0 \left(\frac{\mu}{\mu'}\right)^2 + \lambda_1 \cos\varphi + \lambda_2 \cos 2\varphi + \cdots \ . \tag{5}$$

φ is enclosed by **n** and **c** as the molecular tilt is directed towards the boundary. This expression is valid for circular forms where the electrostatic forces isotropically act in all directions and μ only affects the isotropic line tension and is approximate for regular faceted forms.

When μ increases or the isotropic line tension, λ_0, decreases, the anisotropic terms gain in weight. This means that the boundary energy depends to a larger extent on the orientation of the molecules at the boundary as expressed by the cosine terms. The formation of facets can now be explained by taking a negative λ_1 and zero λ_2. As μ gradually increases (or as λ_0 decreases) the boundary energy is minimised by reducing the curvature of the boundary and the angle between the boundary normal, **n**, and the molecular tilt direction. In the final faceted state the molecules are aligned perpendicularly to the boundary and φ is zero.

On forming a regular hexagon from a circle with six segments the defect line energy rises by 10%, but as faceting is complete, its contribution to the domain shape seems to be of minor importance.

With AA the addition of a trace of cholesterol, which reduces the line tension [19], has the same effect as the increase in pH; a small amount of cholesterol was necessary to get faceted domains of the methyl ester. Firstly, this demonstrates the equivalence of a decrease in line tension with an increase in μ and, secondly, that the faceting of domains, being governed by these forces, is a process under equilibrium. Finally, it illustrates the extent to which domain shapes can be manipulated by impurities, especially if they posses a high affinity for the LC phase-domain boundary. According to this idea, cholesterol seems to affect only λ_0 and not λ_1 or at least only weakly.

If a monolayer of ESD is exposed to an atmosphere containing *n*-heptane, stable faceted forms are observed in the coexistence region [29]. At the saturation pressure of *n*-heptane the domains become dendritic. The shape transformation is a sign that the alkane is incorporated into the monolayer. With the heptane atmosphere an intermediate state between the air-water and the oil-water interface is produced. The difference between the LE and the LC phase vanishes passing from the air-water to the oil-water interface. Correspondingly the line tension becomes smaller on increasing the heptane partial pressure which leads to domain faceting at low pressure and to the formation. According to GID[2]

---

[2] G1D: X-ray diffraction at grazing incidence (Gracing Incidence X-ray Diffraction, also GIXD)

measurements the tilt angle of the AA molecules grows strongly on increasing the pH from 12.0 (from 20° at pH 12.0 to 28° at pH 13, 20 mN m^{-1}, 25 °C) [30]. An increase in the tilt angle diminishes the contact area and the attractive interactions between the chains. The reduced attraction should be reflected by a lower line tension due to a lower expense in energy for breaking bonds and transferring molecules to the interface. Thus, the faceting of AA could be caused by a decrease in the line tension with increasing pH. An indication of the lower effective line energy at pH 12.3 compared to pH 12.0 is the smaller relaxation velocity observed.

The domains of AA at pH 12.0 that were grown under high supersaturation do not display preferred growth directions. This means that anisotropy, which is the prerequisite of dendritic growth [31] and which results in an angular dependence of the growth velocity, is not noticeable. The irregular shape is produced by limited mass transport during the growth process. The boundary smooths immediately after compression has stopped, which indicates a strong line tension and possibly low viscous forces. If the line tension were small, a fractal pattern should be expected, as is usual for isotropic fluids. In contrast AA at pH 12.3 and with the same compression conditions exhibits significant anisotropy and grows with dendrites. What is the reason for dendrites developing and running along the defect lines in this case and along the middle of a segment in the case of ESD? Dendritic growth at low compression rates and almost crystalline behaviour are frequently observed when strong binding forces exist between the molecules, for example, hydrogen bonding in dendritic amides [32]. Growth of dendrites should be preferred in those directions where the attachment of molecules is connected with a lower energy barrier or a higher gain in energy. There are indications from X-ray measurements that in ESD directly neighbouring molecules are bonded more strongly in the direction of tilt than in other directions [22, 33]. This would explain why with ESD the dendrites preferentially grow from the segment middle in the tilt direction. For AA, however, this explanation cannot be applied. If there were enhanced crystallinity in certain directions, dendrites should already appear at pH 12.0.

According to the idea presented above, the ratio of anisotropic-to-isotropic line tension has to increase from pH 12.0 to 12.3 in order to produce facets. Since at pH 12.0 growth appears to be isotropic, the ratio will be small; however, at pH 12.3 the isotropic line tension has reduced so far that dendrites appear that are probably favoured by the anisotropic line tension.

The tendency of having the molecules aligned normal to the boundary is accounted for best when the dendrites run along the segment edges. The worst case is given when the dendrites develop from the segment middle and an arbitrary distribution of cusps, as in the isotropic case, corresponds to the case in-between. To prove this assumption, the line energy was calculated numerically on the basis of Eq. (3), neglecting the second anisotropic term. For this purpose the two extreme cases of dendrite formation were represented by a simple cosine function laid over a circle (Fig. 9). Cases 1 and 2 correspond to the domains in Fig. 8b and c and differ only in the relative orientation of the segments with respect to the dendrites. It is demonstrated that case 1 is more favourable than case 2 and that the difference in line energy between the two cases strongly depends on the ratio between isotropic and anisotropic line tension. If the isotropic line tension is high enough, the difference becomes negligible and the anisotropy of the line tension is not noticeable anymore. For case 1 the length of the defect lines and hence the defect line energy is larger than for case 2. For AA, which corresponds to case 1, the increase in energy for prolonging the defect lines along the dendrites must be lower than the gain in boundary energy due to the anisotropy. As already mentioned, the magnitude of the defect line energy seems to be too low for it to be able to compete with the boundary energy terms.

Conclusion

Under defined experimental conditions faceted monolayer domains were obtained with different substances. A general explanation of facet formation in monolayers

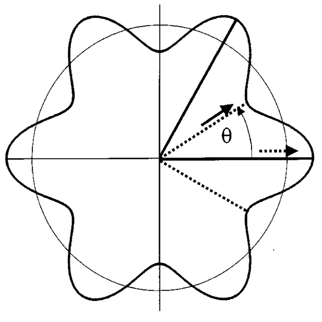

Fig. 9 The sketch represents the nonequilibrium domains of Fig. 8b (segment included by *solid lines*, case 1) and Fig. 8c (*dotted lines* as segment edges, case 2) The boundary is a cosine function laid over a circle with $x = \cos\varphi\,(1 + 0.2\cos 6\varphi)$, $y = \sin\varphi\,(1 + 0.2\cos 6\varphi)$ and $0 \leq \varphi < 2\pi$. $F_\lambda = \int(\lambda_0 + \lambda_1 \mathbf{c}\cdot\mathbf{n})\mathrm{d}l$ with $\lambda_1 < 0$ was chosen as the boundary energy. In case 1 the tilt azimuthal angle, θ, is 30° with respect to the x-axis (*solid arrow*) and in case 2 it is 0° (*dotted arrow*). Integration result: $F_\lambda = 8.16\lambda_0 + 7.2\lambda_1$ (case 1) and $F_\lambda = 8.16\lambda_0 + 4.8\lambda_1$ (case 2); so there can be a remarkable energy difference between case 1 and 2 when an anisotropic line energy is present favouring growth at the segment edges. Normalising against the isotropic line energy $F_\lambda^{\mathrm{iso}} = 8.16\lambda_0$ yields $\Delta F/F_\lambda^{\mathrm{iso}} = 0.29\ \lambda_1/\lambda_0$. The relative energy difference between the two cases vanishes linearly with the ratio of anisotropic-to-isotropic line tension and the anisotropy becomes less important as λ_0 is increased. Then cusps develop arbitrarily and isotropic growth is observed

is offered in which it is assumed that the molecules in the monolayer must be tilted and that the domains must be divided into segments of uniform tilt for facets to appear. The basic force is the line tension anisotropy that expresses the tendency of the molecules at the domain boundary to adopt a certain orientation. The origin of this "boundary pinning force" is unclear. It is perhaps caused by dipoles in the monolayer plane and it is presumably not connected with the presence of the LE phase, since with cholesterol, which induces faceting of domains of AA at pH 12.0, the boundary is probably screened off by attached molecules. Faceting is observed when the isotropic line tension that counteracts a lengthening of the boundary is reduced far enough or, equivalently, when the dipolar repulsion is increased. This concept can also be applied to explain the preferred dendrite formation along segment edges, which besides being observed for AA was also observed in the methyl ester (Fig. 6c, d). Hence the line tension anisotropy also affects the branching pattern of the stripes (Fig. 6e). Knowing about the forces that determine the domain shape, domains can serve as an indicator for processes and conditions in and at the monolayer, such as incorporation of molecules from the gas or the subphase and also for desorption changing the chemical composition within the domain, for the presence of impurities or the reaction of the subphase with the monolayer, such as headgroup dissociation or screening, or for the cleavage of groups or reorientations that lead to a change in μ.

Acknowledgements Financial assistance from the Deutsche Forschungsgemeinschaft (Sfb 312) and the Fonds der Chemischen Industrie is gratefully acknowledged.

References

1. Keller DJ, Korb JP, McConnell HM (1987) J Phys Chem 91:6417
2. Langer SA, Goldstein RE, Jackson DP (1992) Phys Rev A 46:4894
3. Qiu X, Ruiz-Garcia J, Stine KJ, Knobler CM (1991) Phys Rev Lett 67:703
4. Fischer TM, Bruinsma RF, Knobler CM (1994) Phys Rev E 50:413
5. Nelson DR, Halperin BI (1980) Phys Rev B 21:5312
6. Ho TL (1992) In: Strandburg K (ed) Bond-orientational order in condensed matter systems. Springer, Berlin Heidelberg New York, pp 216–254
7. Lösche M, Duwe HP, Möhwald H (1988) J Colloid Interface Sci 126:432
8. McConnell HM (1991) Annu Rev Phys Chem 42:171
9. Vanderlick TK, Möhwald H (1990) J Phys Chem 94:886
10. Seul M, Sammon MJ (1990) Phys Rev Lett 64:1903
11. Heckl WM, Möhwald H (1986) Ber Bunsenges Phys Chem 90:1159
12. Langer SA, Sethna JP (1986) Phys Rev A 34:5035
13. Rivière S, Meunier J (1995) Phys Rev Lett 74:2495
14. Fischer B, Tsao MW, Ruiz-Garcia J, Fischer TM, Schwartz DK, Knobler CM (1996) Thin Solid Films 284–285:110–114
15. Loh KK, Rudnick J (1998) Phys Rev Lett 81:4935
16. Johann R, Vollhardt D (1999) Mater Sci Eng C (in press)
17. Oishi Y, Takashima Y, Suehiro K, Kajiyama T (1997) Langmuir 13:2525
18. Helm CA, Laxhuber L, Lösche M, Möhwald H (1986) Colloid Polym Sci 264:46
19. Weis RM, Mc Connell HM (1985) J Phys Chem 89:4453
20. Vollhardt D, Gehlert U (1996) Tenside Surf Det 33:197
21. Miller A, Helm CA, Möhwald H (1987) J Phys 48:693
22. DeWolf C, Bringezu F, Brezesinski G, Möhwald H, Howes P, Kjaer K (1998) Physica B 248:199
23. Berge B, Faucheux L, Schwab K, Libchaber A (1991) Nature 350:322
24. Costas ME, Knobler CM (1992) Rev Mex Fis 38:791
25. Dietrich A, Brezesinski G, Möhwald H, Dobner B, Nuhn P (1994) Nuovo Cimento 16D:1537
26. Qiu X, Ruiz-Garcia J, Knobler CM (1992) Prog Colloid Polym Sci 89:197
27. Andelmann D, Brochard J, Joanny JF (1987) J Chem Phys 86:3673
28. Patil GS, Matthews RH, Cornwell DG (1972) J Lipid Res 13:574
29. Harke M, Motschmann H (1998) Langmuir 14:313
30. Johann R, Vollhardt D, Weidemann G (1998) HASYLAB DESY annual report, Hamburg, p 419
31. Nittmann J, Stanley HE (1986) Nature 321:663
32. Melzer V, Weidemann G, Vollhardt D, Brezesinski G, Wagner R, Struth B, Möhwald H (1997) Supramol Sci 4:391
33. Gehlert U (1996) PhD thesis. Technische Universität, Berlin